therefore submicrometer structures should be possible, especially when photochemically enhanced processes are used instead of purely thermal growth. The latter was used here because it allows a high growth rate (up to 100 μm/s).

REFERENCES AND NOTES

1. E. Yablonowitch, *Phys. Rev. Lett.* **58**, 2059 (1987).
2. O. Lehmann and M. Stuke, *Science* **270**, 1644 (1995) and references therein.
3. E. Yablonowitch *et al.*, *Phys. Rev. Lett.* **67**, 3380 (1991) and references therein.
4. Special issues of *J. Opt. Soc. Am.* **B10**, no. 2 (1993) and *J. Mod. Opt.* **41**, 171 (1994); C. M. Soukoulis, Ed., *Photonic Band Gap Materials* (Kluwer Academic, Dordrecht, Netherlands, 1996).
5. E. Özbay *et al.*, *Opt. Lett.* **19**, 1155 (1994). See also other publications from this group.
6. U. Grüning, V. Lehmann, S. Ottow, K. Busch, *Appl. Phys. Lett.* **68**, 747 (1996); A. Rosenberg *et al.*, *Opt. Lett.* **21**, 830 (1996).
7. F. T. Wallenberger, *Science* **267**, 1274 (1995) and references therein.
8. M. Boman, H. Westberg, S. Johansson, J.-Å. Schweitz, *Proceedings of the 5th International Workshop on Micro Electro Mechanical Systems*, Travemünde, Germany, 4 to 7 February 1992 (Institute of Electrical and Electronics Engineers, Piscataway, NJ, 1992).
9. O. Lehmann and M. Stuke, *Mater. Lett.* **21**, 131 (1994).
10. V. N. Bogomolov *et al.*, *Appl. Phys.* **A63**, 617 (1996).
11. E. Özbay and B. Temelkuran, *Appl. Phys. Lett.* **69**, 743 (1996).
12. H. Hirayama, T. Hamano, Y. Aoyagi, *ibid.*, p. 791.

13. We thank U. Biermann (Philips Eindhoven) for support; H. Hahn and his group at the Technische Hochschule (TH) Darmstadt, D. Clark, and Y. Li for x-ray measurements; and Bundesministerium für Bildung, Wissenschaft, Forschung und Technologie (grant 13 N 6159 7), the European Research Office (grant USARDSG-UK), and NSF for financial support.

6 September 1996; accepted 18 December 1996

Low-Temperature Nonoxidative Activation of Methane over *H*-Galloaluminosilicate (MFI) Zeolite

Vasant R. Choudhary,* Anil K. Kinage, Tushar V. Choudhary

Conversion of methane to higher hydrocarbons by its low-temperature activation without forming undesirable carbon oxides is of great scientific and practical importance. Methane can be highly activated, yielding high rates of conversion to higher hydrocarbons and aromatics (10 to 45 percent) at low temperatures (400° to 600°C), by its reaction over *H*-galloaluminosilicate ZSM-5 type (MFI) zeolite in the presence of alkenes or higher alkanes. The methane activation results from its hydrogen-transfer reaction with alkenes.

Methane, the most inert of hydrocarbons, has been extremely difficult to activate for direct conversion to higher hydrocarbons. In the past 10 to 12 years, some success has been achieved by oxidative coupling of methane (OCM) to ethane and ethylene over a number of basic catalysts in the presence or absence of free oxygen (*1–4*) and over pentasil zeolites with nitrous oxide as the oxidant (*5*). In the OCM process, the selectivity for higher hydrocarbons is high only at low conversion rates. Moreover, this process involves formation of undesirable products such as CO_2 and CO because of the highly exothermic hydrocarbon combustion reactions, which can also be hazardous. More recently, a dehydrogenative coupling of methane to ethane over active carbon was reported (*6*). However, the temperature required for methane activation by its dehydrogenative coupling is very high (≥1100°C).

Our new approach for obtaining high rates of conversion of methane to higher hydrocarbons, without formation of carbon oxides and at much lower temperatures (400° to 600°C), involves nonoxidative activation of methane by hydrogen-transfer reactions between methane and alkene over H-GaAlMFI zeolite. The zeolite is a bifunctional catalyst with strong acid sites (because of the tetrahedral Al and Ga in the zeolite framework) as well as dehydrogenation functions (because of a combination of zeolitic protons and extra framework Ga-oxide species).

To illustrate this approach, we converted methane to higher hydrocarbons (or aromatics) over the zeolite through the addition of C_2 to C_4 alkenes, propane, or *n*-hexane in the feed. The zeolite was prepared and characterized by procedures similar to those in (*7*). Catalytic reactions were carried out at ambient pressure in a continuous-flow tubular reactor (*8*, *9*). The reactor (internal diameter, 13 mm) was made of quartz. A mixture of N_2 (>99.99%), methane (99.95%), and alkene or higher alkane (>99.5%) was passed over the zeolite catalyst (1 g) for a period of ~5 min at different feed compositions and temperatures. The square pulse technique previously described (*9*) was used. The space velocity of the feed gas mixtures was measured at 0°C and 1 atm. The conversion and product selectivity data were obtained from the feed and product composition as follows:

Conversion (%)

$$= \left[\frac{\begin{array}{c}\text{(weight \% of reactants}\\\text{in the feed hydrocarbons)} -\\\text{(weight \% of reactants in the}\\\text{product hydrocarbons)}\end{array}}{\begin{array}{c}\text{weight \% of reactants in}\\\text{the feed hydrocarbons}\end{array}}\right] \times 100 \tag{1}$$

Product selectivity (%)

$$= \left[\frac{\begin{array}{c}\text{weight \% of the product}\\\text{in the hydrocarbon products}\end{array}}{\begin{array}{c}100 - \text{(weight \% of reactants}\\\text{in the hydrocarbon products)}\end{array}}\right] \times 100 \tag{2}$$

The conversion of feed hydrocarbon (or hydrocarbons) to carbon (coke on the catalyst) was found to be ≤1 weight %. The carbon and hydrogen balances in the reactions were within 3 to 7%.

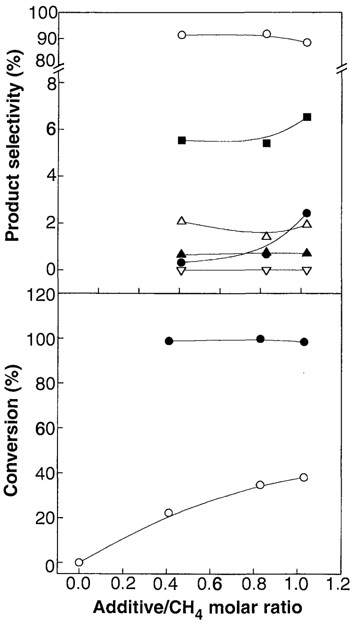

Fig. 1. Effect of the propene/methane molar ratio in feed on the conversion of methane (○) and propene (●) and the selectivity for aromatics (○), ethene (△), ethane (▲), propane (■), C_4 (●), and C_{5+} (▽) aliphatics in the simultaneous aromatization of methane and propene over *H*-GaAlMFI zeolite at 500°C (concentration of methane in feed, 33.3 mol %; space velocity, 6200 cm^3 g^{-1} $hour^{-1}$).

Chemical Engineering Division, National Chemical Laboratory, Pune 411 008, India.

*To whom correspondence should be addressed. E-mail: vrc@ncl.ernet.in

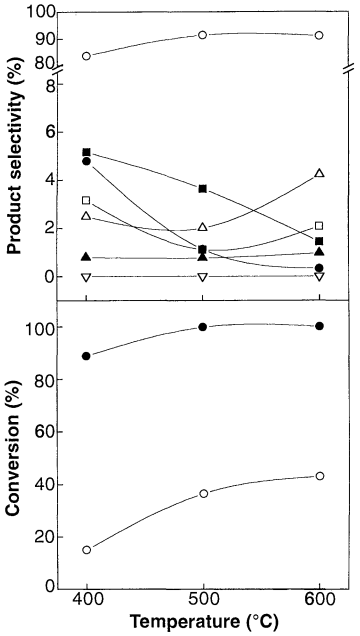

Fig. 2. Effect of temperature on the conversion of methane (○) and *n*-butene (●) and on the selectivity for aromatics (○), ethene (△), ethane (▲), propene (□), propane (■), butane (●), and C_{5+} (▽) aliphatics in the simultaneous aromatization of methane and *n*-butene over *H*-GaAlMFI zeolite (n-C_4H_8/CH_4 molar ratio, 0.45 ± 0.03; concentration of CH_4 in feed, 33.3 mol %; space velocity, 6200 $cm^3\ g^{-1}\ hour^{-1}$).

Table 1. Results for the aromatization of methane over *H*-GaAlMFI zeolite in the presence of different additives (alkenes or higher alkanes) in the feed (a mixture of CH_4, N_2, and additive; concentration of methane in feed, 33.3 mol %).

Additive in feed	Additive/ CH_4 molar ratio	Space velocity ($cm^3\ g^{-1}\ hour^{-1}$)	Temp. (°C)	Conversion (%)		Selectivity for aromatics (%)
				CH_4	Additive	
None	0.0	3100	600	0.0	–	–
None	0.0	6200	600	0.0	–	–
n-Butene	0.5	3100	600	45.0	100	92.0
i-Butene	0.5	6200	500	44.2	100	93.8
Propene	0.8	6200	500	34.7	99.7	91.8
Ethene	1.0	6200	600	36.3	98.8	93.8
Propane	0.7	3100	600	12.0	91.1	84.2
n-Hexane	0.8	3100	600	24.1	100	93.8

Table 2. Comparison of the results of aromatization of *n*-butene, propene, and ethene over *H*-GaAlMFI zeolite in the presence and absence of methane in the feed (a mixture of alkene and pure N_2 with or without methane; concentration of alkene in feed, 33.3 mol %; space velocity of gaseous mixture, 6200 $cm^3\ g^{-1}\ hour^{-1}$).

Hydrocarbons in feed	Methane/ alkene molar ratio	Temp. (°C)	Conversion of alkene (%)	Methane conversion (%)		Selectivity for aromatics (%)	H_2 produced ($dm^3\ g^{-1}\ hour^{-1}$)	
				From feed and product composition	From methane balance*		Estimated†	Observed‡
n-C_4H_8	0.0	500	100	–	–	89.3	2.82	2.90
n-$C_4H_8 + CH_4$	1.0	500	100	33.0	35.3	92.4	3.88	3.72
C_3H_6	0.0	550	100	–	–	90.1	1.98	2.15
$C_3H_6 + CH_4$	1.0	550	100	36.2	32.1	90.7	3.22	3.09
C_2H_4	0.0	550	95.8	–	–	91.1	1.33	1.48
$C_2H_4 + CH_4$	1.0	550	94.2	29.0	31.2	94.5	2.27	2.4

*Methane conversion = [(flow rate of methane in the feed) − (flow rate of methane in the products)/flow rate of methane in the feed] × 100. †H_2 produced is estimated from the composition of hydrocarbons in the feed and products. ‡H_2 produced is obtained directly from the knowledge of the flow rate of gaseous products and their composition.

High rates of conversion of methane into higher hydrocarbons or aromatics occured over the zeolite in the presence of alkenes or higher alkanes in the feed (Tables 1 and 2 and Figs. 1 and 2). The zeolite showed no activity for methane conversion at ≤600°C in the absence of alkenes or higher alkanes. However, the addition of alkenes or higher alkanes in the feed increased methane conversion from 0 to ≤45%, depending on the additive (alkene or higher alkane), the additive/CH_4 molar ratio in the feed, and the temperature. More methane conversion occurred at higher additive/CH_4 ratios (Fig. 1) and at higher temperatures (Fig. 2). The selectivity for aromatics in the simultaneous aromatization of methane and alkenes or higher alkanes was also very high.

Rates of conversion of methane to higher hydrocarbons as high as ~45%, without formation of carbon oxides, could be obtained by the addition of isobutene or *n*-butene (Table 1) in the feed. Such a high yield of higher hydrocarbons from methane in a single pass has not been obtained with the OCM process, even at much higher temperatures (≥800°C).

The ZSM-5 zeolites show high activity for the hydrogen-transfer reaction between alkane and alkene, even at 400°C (*10*). The low-temperature nonoxidative activation of methane is expected mostly because of hydrogen-transfer reactions between alkane and alkene over the bifunctional zeolite, involving the following elementary reaction steps:

$$C_nH_{2n} + H^+ \leftrightarrow (C_nH_{2n+1})^+ \qquad (3)$$

$$\begin{array}{c} H—CH_3 \\ + \\ —Ga—O— \end{array} \rightarrow \begin{array}{ccc} H^{-\delta} & ---- & CH_3{}^{+\delta} \\ : & & : \\ —Ga & —— & O— \end{array} \qquad (4)$$

$$(C_nH_{2n+1})^+ + \begin{array}{ccc} H^{-\delta} & ---- & CH_3{}^{+\delta} \\ : & & : \\ —Ga & —— & O— \end{array}$$

$$\rightarrow C_nH_{2n+2} + CH_3{}^+ \qquad (5)$$

$$CH_3{}^+ \rightarrow CH_2 + H^+ \qquad (6)$$

$$2CH_2 \rightarrow C_2H_4 \qquad (7)$$

Thus, the overall reaction involved in the methane activation is

$$2CH_4 + 2C_nH_{2n} \rightarrow 2C_nH_{2n+2} + C_2H_4 \qquad (8)$$

The conversion of methane in the presence of isobutene over *H*-ZSM-5 (Si/Al = 13.6) at 600°C was negligibly small, but its conversion over *H*-ZSM-5 zeolite containing nonframework Ga-oxide species (namely, Ga/*H*-ZSM-5) was appreciable. Hence, methane activation in the presence of alkene over the *H*-GaAlMFI zeolite is expected to occur over the nonframework Ga-oxide species (Eq. 4). The C–H bond cleavage, however, takes place only by the hydride transfer from the partially activated methane to the carbonium ion (Eq. 5). The methylinium ion ($CH_3{}^+$) formed in this reaction is rapidly decomposed (Eq. 6) and releases the proton and CH_2 radical; the latter is rapidly dimerized to ethene (Eq. 7). In the absence of alkene, no conversion of methane over the *H*-GaAlMFI zeolite was observed. Therefore, the presence of a carbonium ion is essential for the cleavage of the C–H bond of methane.

Because of its very high reactivity, the higher alkane formed in Eq. 5 undergoes fast dehydrogenation over the zeolite, thus regenerating the alkene consumed in the hydrogen-transfer reaction:

$$C_nH_{2n+2} \xrightarrow{H^+ + \text{Ga-oxide}} C_nH_{2n} + H_2 \qquad (9)$$

The ethene and higher alkenes are oligomerized and then dehydrocyclized to aromatics over the bifunctional zeolite catalyst:

$$C_2 \text{ to } C_4 \text{ alkenes} \overset{H^+}{\rightarrow} C_6 \text{ to } C_{10} \text{ alkenes}$$

$$\xrightarrow{H^+ + \text{Ga-oxide}} \text{aromatics} \qquad (10)$$

The methane activation resulting from the presence of the higher alkane also involves the above reactions, but the alkane is first converted to alkene by Eq. 9.

Because of the very large change in free energy ($\Delta G_r > 48$ kcal/mol of benzene) that would be involved, the direct formation of benzene from methane at ≤600°C is thermodynamically impossible. However, the thermodynamic barrier is drastically reduced or even eliminated as a result of the addition of alkenes or higher alkanes; the value of ΔG_r approaches zero or even becomes negative, depending on the additive, its concentration relative to that of methane, and the temperature. For example, for an *n*-butene/methane ratio of 1.0, $\Delta G_r = -4.1$ kcal/mol at 500°C and -10.6 kcal/mol at 600°C (*11*).

According to the stoichiometry of Eq. 8 (which is responsible for the methane activation), the rate of methane conversion should increase with an increasing alkene/CH_4 ratio. The results in Fig. 1 are consistent with this assumption. Further, the appreciable formation of butanes from *n*-butene, particularly at lower temperatures (Fig. 2), and that of propane from propene (Fig. 1), also indicate the occurrence of the hydrogen-transfer reaction. The observed high methane activation (at lower temperature and higher space velocity) resulting from the isobutene additive (Table 1) is consistent with the *tert*-butyl carbonium ions being more stable than the primary and secondary butyl carbonium ions. This interpretation also supports the involvement of carbonium ions in the methane activation by Eq. 5.

A comparison of the results of alkene aromatization in the presence of methane with that in the absence of methane (Table 2) shows a marked increase in H_2 production in the reaction when methane is present in the feed; the observed flow rate of the H_2 formed is quite close to that estimated from the composition of feed and products. Moreover, the methane conversion values estimated from the feed and product compositions are quite close to that obtained directly from the methane flow measured at the inlet and outlet of the reactor. Also, in general, there is a small but appreciable increase in the selectivity for aromatics because of the presence of methane (Table 2). All of these observations confirm the low-temperature methane activation over the zeolite as a result of the presence of the additives.

Our results show that methane can be highly activated, and hence converted to higher hydrocarbons and aromatics with high conversion rates at low temperatures (≤600°C), by its hydrogen-transfer reactions with alkenes over the zeolite. This method could provide an environmentally cleaner process, operating at much lower temperatures, for converting methane into higher hydrocarbons without the formation of undesirable carbon oxides.

REFERENCES AND NOTES

1. J. S. Lee and S. T. Oyama, *Catal. Rev. Sci. Eng.* **30**, 249 (1988).
2. G. J. Hutchings, J. R. Woodhouse, M. S. Scurrel, *Chem. Soc. Rev.* **18**, 251 (1989).
3. Y. Amenomiya, V. I. Birss, M. Goledzinowski, J. Galuszka, A. R. Sanger, *Catal. Rev. Sci. Eng.* **32**, 163 (1990).
4. J. H. Lunsford, *Catal. Today* **6**, 235 (1990); *Angew. Chem. Int. Ed. Engl.* **34**, 970 (1995).
5. S. S. Shepelev and K. G. Ione, *J. Catal.* **117**, 362 (1989).
6. H. Yagita *et al.*, in *Environmental Catalysis*, G. Centi, C. Cristiani, P. Forzatti, S. Perathoner, Eds. (SCI, Rome, 1995), pp. 639–642.
7. V. R. Choudhary, A. K. Kinage, C. Sivadinarayana, M. Guisnet, *J. Catal.* **158**, 23 (1996).
8. For the zeolite, framework (FW) Si/Ga = 49.9, FW Si/Al = 40.3 (with no non-FW Al), Na/(Al + Ga) = 0.03, and non-FW Ga = 0.32 mmol g^{-1}; strong acid sites (measured by the chemisorption of pyridine at 400°C) = 0.46 mmol g^{-1}; and size of spherical-hexagonal crystals = 5.5 ± 1.5 μm.
9. V. R. Choudhary *et al.*, *J. Catal.* **158**, 34 (1996).
10. D. B. Lukynov, *ibid.* **145**, 54 (1994); *ibid.* **147**, 494 (1994).
11. See the supplementary table at *Science*'s World Wide Web site (http://www.sciencemag.org) for ΔG_r and ΔH_r values for different methane aromatization reactions.

12. A.K.K. thanks the Council of Scientific and Industrial Research, New Delhi, for a senior research fellowship.

11 November 1996; accepted 2 January 1997

Dissociation of Methane into Hydrocarbons at Extreme (Planetary) Pressure and Temperature

F. Ancilotto, G. L. Chiarotti,* S. Scandolo, E. Tosatti

Constant-pressure, first-principles molecular dynamic simulations were used to investigate the behavior of methane at high pressure and temperature. Contrary to the current interpretation of shock-wave experiments, the simulations suggest that, below 100 gigapascals, methane dissociates into a mixture of hydrocarbons, and it separates into hydrogen and carbon only above 300 gigapascals. The simulation conditions (100 to 300 gigapascals; 4000 to 5000 kelvin) were chosen to follow the isentrope in the middle ice layers of Neptune and Uranus. Implications on the physics of these planets are discussed.

The high-pressure and high-temperature behavior of methane (CH_4), the most abundant organic molecule in the universe, is of great importance in planetary physics. Current models (*1*, *2*) of the interiors of Neptune and Uranus are based on the existence of a middle ice layer made of CH_4, NH_3, and H_2O in solar proportions. In this layer, pressure and temperature (*P*-*T*) range from 20 GPa and 2000 K to 600 GPa and 8000 K. Shock-wave experiments indicate that, in spite of its stability at ambient conditions (*3*), CH_4 dissociates at these extreme conditions (*4*), possibly into H_2 and carbon, with precipitation of solid diamond (*5*). Here we present computer simulations that show a different, more complex, chemical breakdown.

The lack of direct information on the interior structure of Neptune and Uranus has restricted attempts to understand the behavior of CH_4 under extreme pressures to the interpretation of laboratory-based shock-wave experiments (*4*), where planetary *P*-*T* conditions are achieved. An alternative tool for such an investigation is computer simulation (*6*). Our simulations are based on a recently developed deformable-cell method for constant-pressure, first-principles molecular dynamics (*7*).

We set our simulation conditions at 100 GPa and 4000 K (*8*), which correspond to the *P*-*T* conditions at a distance of about two-thirds of the planetary radius from the center. This pressure is also the highest reached in shock-wave experiments (*4*). In the first picosecond of the simulation, the initial configuration of 16 CH_4 molecules (Fig. 1A) under-

F. Ancilotto, Dipartimento di Fisica "G. Galilei," Universitá di Padova, Via Marzolo 8, I-35131 Padova, and Istituto Nazionale di Fisica della Materia, Italy.
G. L. Chiarotti, International School for Advanced Studies (SISSA), Via Beirut 4, I-34014 Trieste, and Istituto Nazionale di Fisica della Materia, Italy.
S. Scandolo and E. Tosatti, SISSA, Via Beirut 4, I-34014 Trieste, International Centre for Theoretical Physics, I-34014 Trieste, and Istituto Nazionale di Fisica della Materia, Italy.

---

*To whom correspondence should be addressed. E-mail: guido@sissa.it